

Automatic Densitometer Measurements of Powder Diffraction Photographs

GUNNAR MALMROS and PER-ERIK WERNER

*Institute of Inorganic and Physical Chemistry, University of Stockholm,
S-104 05 Stockholm 50, Sweden*

The use of an automatic drum densitometer for the evaluation of powder diffraction photographs is described. Computer programs for the calculation of Bragg angles and diffraction intensities from Guinier-Hägg photographs have been constructed. The speed and accuracy of the technique are discussed and illustrated by examples.

Due to the availability of automatic drum film scanners, it is possible to make fast routine determinations of interplanar spacings and diffraction intensities from X-ray powder photographs. Accuracy in low-order lines is of great importance when the high-angle region is too crowded or too weak to be of any use for indexing complicated patterns or measuring lattice constants. A vast number of research problems falls into these categories and it has been found that powder photographs obtained in a focusing camera of the Guinier-Hägg type and measured by a precision method described by Hägg¹ and Westman and Magnéli² give results satisfactory for most needs. The use of an internal standard with known cell constants makes it possible in principle to attain a precision limited by the instrumental inaccuracy and the precision of the lattice parameters of the standard. However, the application of the method is often tiresome, and subjective errors in reading and operating may well be introduced. The use of an automatic film scanner offers a possibility of avoiding subjective errors and of giving more satisfactory intensity measurements than the frequently used visual estimations: *very strong*, *strong*, *medium*, *weak*, *very weak* and *very very weak*. Furthermore in favourable situations, *e.g.* where there are only small orientation effects in the specimen, it may be possible to measure the intensities with an accuracy comparable with that obtained with a single-crystal Weissenberg camera (*cf.* Table 3). It is also well known that fine powders can be ideal subjects for accurate intensity measurements because of the virtual absence of both primary and secondary extinction in most cases.³

FILM SCANNER PROCESS

The drum scanner used in the present work is an automatic film scanner SAAB model 2,⁴ designed by Abrahamsson.⁵ A special film cassette for Guinier photographs was designed. In this cassette the film is mounted with the powder lines perpendicular to the film scanner drum axis. The film is pierced with a needle close to the primary beam streak in order to facilitate the automatic indexing of the lines from the standard. The scanner is connected to an IBM 1800 computer.⁶ A block diagram of the film scanner process is given in Fig. 1.

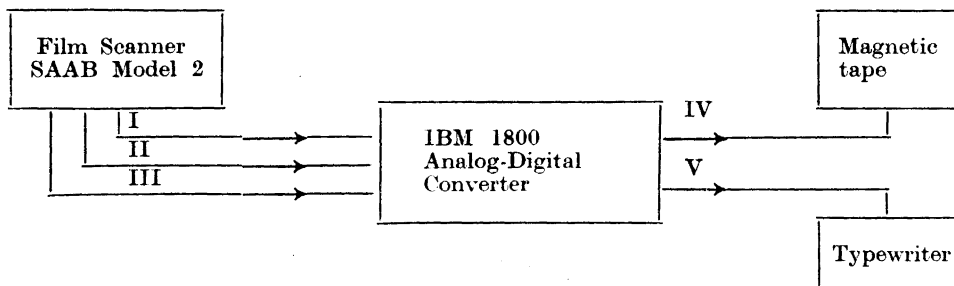


Fig. 1. Film scanner process block diagram. I. Process interrupt (about 3 times/sec). II. Analog output of transmission values. III. Synchronization pulses at each $60\text{ }\mu\text{m}$ film translation. IV. Digital transmission values. V. System messages.

The process programs, written in IBM 1800 Assembler Language,⁷ are executed on-line under the IBM 1800 Multiprogramming Executive System, MPX.⁸ At the present stage the following equipment is available: a 32 K core memory, a card read-punch station, a line printer, a console typewriter, a magnetic tape unit and two disk drives. By the use of data-channels the need for central process unit time is reduced to only a few per cent of the total scan time, which latter is about 10 min for the measuring of one Guinier photograph. This means that non-process programs or other programs of lower priorities which do not need the magnetic tape unit may be executed simultaneously without any considerable loss of speed.

It should be noted that the SAAB scanner produces transmission values and not optical densities, contrary to other drum film scanners available on the market. It has been found that the *positions* of the lines are more easily detected and measured on a transmission curve than on an intensity curve (*cf.* Fig. 3).

Each revolution of the film scanner drum corresponds to a translation of $45\text{ }\mu\text{m}$ along the drum axis and produces one magnetic tape record of 266 transmission values, *i.e.* $266 \times 60\text{ }\mu\text{m} = 15.96\text{ mm}$ on the photograph parallel to the powder lines. By means of the analog digital converter (*cf.* Fig. 1) the transmission values are calculated with a precision of eleven binary digits. Thus a digitized picture of the Guinier photograph is stored on the magnetic tape.

SOFTWARE SYSTEM

In order to calculate interplanar spacings, d , and integrated intensities from the transmission values stored on the magnetic tape, one of us (G. M.) has written the computer program PILT (Powder Intensity and Lattice Tracing) in IBM 1800 Fortran.

In the first step the program evaluates the positions, s , of the lines on the film. The relation between Bragg angles, θ , and s -values is computed by least-squares treatment of the positions of the lines from the standard substance. It has been observed that s as a function of θ is better approximated by a parabolic function (*cf.* Fig. 2 in Ref. 2) than by use of a linear function. This technique is therefore included in the program. In the next step PILT computes integrated intensities and applies the *PLG*-factors, where P , L , and G , are the polarization, the Lorentz, and the geometric factors.

$$P = [1 + \cos^2(2\alpha) \cos^2(2\theta)]/[1 + \cos^2(2\alpha)]$$

where α is the Bragg angle for the monochromator crystal which is assumed to have an ideal mosaic structure.⁹

$$L = 1/\sin^2 \theta \cos \theta$$

and

$$G = 1/\cos(2\theta - \phi)$$

where ϕ is the angle between the normal to the specimen plane and the primary beam.¹⁰ The program also punches data cards for the program PIRUM,¹¹ which performs indexing of powder patterns and refines cell parameters by the method of least-squares.

In calculation of the line positions two problems arise. The first is to distinguish between the diffraction lines and the background variations and the second is to determine the peak positions. The principles used by PILT will now be summarized.

From each revolution of the film scanner drum, corresponding to a $45 \mu\text{m}$ translation along the film, the arithmetic mean T_m of the transmission values from a 2 mm broad slit is calculated (*cf.* Fig. 2). The slit corresponds to 34 single readings by the scanner. This procedure reduces the great amount of data on the tape to a vector of less than 2700 integers which can be kept in core memory. Each integer represents the average transmission, T_m , of $45 \mu\text{m}$ perpendicular to the diffraction lines on the film.

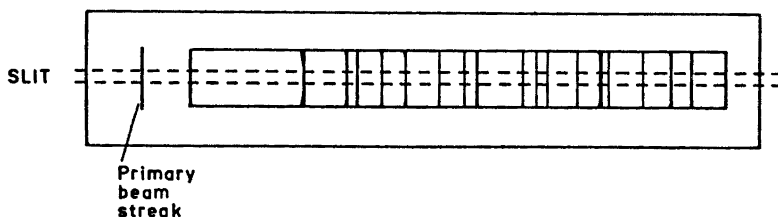


Fig. 2. Schematic drawing of a powder photograph.

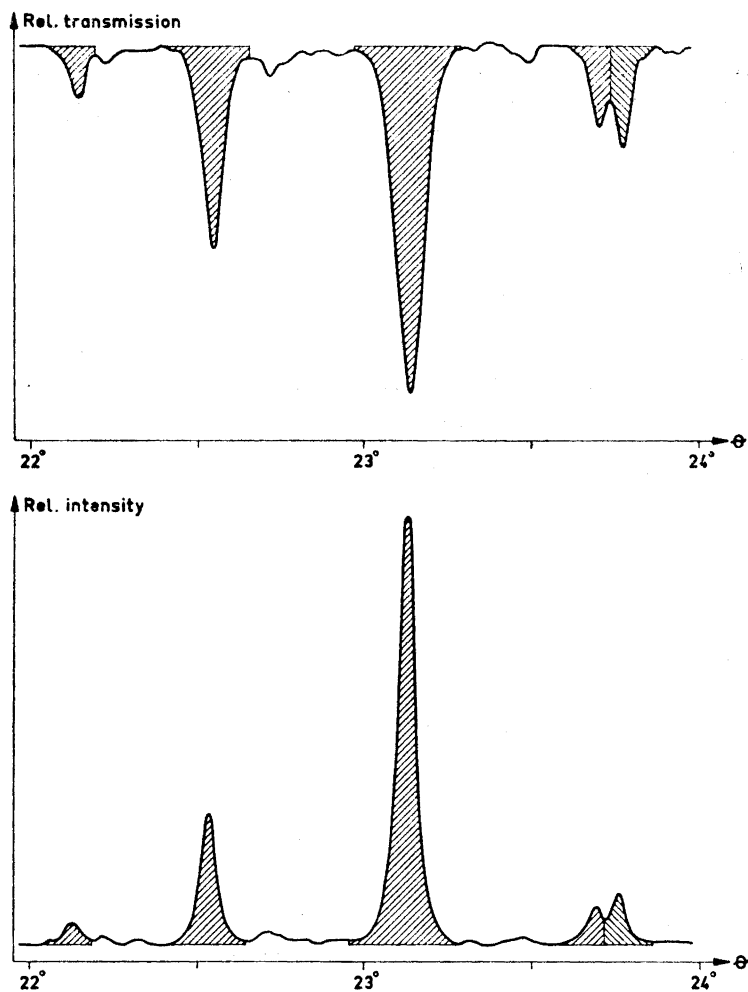


Fig. 3. Parts of corresponding transmission and relative intensity curves derived from a powder photograph of α - Bi_2O_3 .

As can be seen from Fig. 3 the weak lines appear much more clearly on the transmission curve than on the intensity curve. Therefore, the positions of the lines are calculated from the transmission values. For each T_m the derivative dT_m/ds is calculated and it is supposed that a line may be present if dT_m/ds exceeds a certain limit. The position of the line is estimated by linear interpolation to the s -value where $dT_m/ds = 0$. If the difference between the minimum transmission and the transmission value $90\ \mu\text{m}$ (*i.e.* 2 revolutions) away is less than 5 %, the assumed line is discarded. Often this procedure eliminates all

spurious lines. If such "lines" occur they can easily be removed by visual inspection of the transmission curve given on the line printer.

In calculating the integrated intensities it is essential to determine a proper background level. The following procedure is used by the program. For each group of 100 T_m values the 10 consecutive ones giving the highest mean transmission are chosen as the background level. The background, T_b , for each point on the curve is then calculated by linear interpolation.

The width of a peak is defined by revolutions r_1 and r_2 where dT_m/ds is zero or changes sign. In Fig. 3 the shadowed areas represent the integrated intensities

$$I = 100 \times \sum_{i=r_1}^{r_2} D_i'$$

where D_i' are corrected relative optical densities calculated from the equations

$$D_i' = D_i (1 + kD_i)$$

and

$$D_i = \log (T_b/T_m)$$

The correction term kD_i is further discussed in Ref. 12. The value 0.4 is usually suitable for k .

DISCUSSION

The correctness of cell parameters with standard deviations and intensities of powder lines obtained by the technique described above has been tested.

Table 1. Guinier powder pattern of $\text{Pb}(\text{NO}_3)_2$ $\text{CuK}\alpha_1$ radiation, $\lambda = 1.54051 \text{ \AA}$. $\Delta = 10^5 \times (\sin^2\theta_{\text{obs II}} - \sin^2\theta_{\text{calc II}})$.

$ F ^2_{\text{obs}}$	$\sum h^2 + k^2 + l^2$	$\sin^2\theta_{\text{obs I}}$ $\times 10^5$	$\sin^2\theta_{\text{obs II}}$ $\times 10^5$	$\sin^2\theta_{\text{calc II}}$ $\times 10^5$	Δ
1064	3	2875	2875	2884	-8
861	4	3840	3841	3845	-4
187	5	4804	4807	4806	1
153	6	5768	5768	5767	1
1551	8	7688	7690	7690	0
3471	11	10575	10576	10573	2
2043	12	11536	11538	11535	4
1331	16	15387	15386	15380	6
55	18	17305	17312	17302	10
2802	19	18269	18267	18263	4
2682	20	19230	19230	19224	6
2719	24	23078	23076	23069	7
3172	27	25949	25953	25953	0
1808	32	30753	30754	30759	-6
5423	35	33633	33640	33643	-3
2768	36	34605	34600	34604	-4
1434	40	38445	38443	38449	-6
1841	43	41342	41334	41333	1
2175	44	42321	42293	42294	-1

Such tests have been performed by use of photographs from substances of different symmetries.

A powder photograph of $\text{Pb}(\text{NO}_3)_2$ with Si ($a = 5.4301 \text{ \AA}$)¹³ as internal standard was obtained at 25°C by a Guinier-Hägg focusing camera.¹ The photograph was mounted in the film cassette and scanned twice by the drum densitometer. The $\sin^2 \theta$ values derived from the two scans are presented in Table 1. The cell edges with standard deviations of this cubic substance derived by least-squares treatment are 7.8564 (2) Å and 7.8559 (3) Å, respectively. Thus, the reproducibility of the procedure is within two estimated standard deviations. These calculated cell dimensions may also be compared with those obtained by Westman and Magnéli,² 7.8560 (2) Å at 20°C, and by Swanson *et al.*,¹⁴ 7.8568 Å (no standard deviation given) at 25°C.

As mentioned above the θ values are derived by a least-squares treatment of a parabolic function $s = f(\theta)$. It has been found that if a linear dependence of the line positions, s , as a function of θ is assumed, errors in the calculated cell dimensions with an order of magnitude of several standard deviations may occur.

In Table 2 the cell dimensions of MoO_3 derived from film scanner data are compared with the cell parameters obtained by Westman and Magnéli² from careful visual estimation of the same photograph. As can be seen from Table 2

Table 2. Lattice parameters for MoO_3 . Radiation used: $\text{CuK}\alpha_1$, $\lambda = 1.54051 \text{ \AA}$.

Present work	Westman and Magnéli ²
$a = 3.9623 \text{ (3) \AA}$	$a = 3.9628 \text{ (9) \AA}$
$b = 13.858 \text{ (2) \AA}$	$b = 13.855 \text{ (4) \AA}$
$c = 3.6978 \text{ (4) \AA}$	$c = 3.6964 \text{ (8) \AA}$

the standard deviations are significantly diminished by the film scanner technique. It should also be noted that the cumbersome visual estimation of the line positions is reduced to a small number of manual operations of the scanner and that the complete result was achieved within a few minutes after the scan procedure.

The squares of the structure factors derived from a powder specimen of $\alpha\text{-Bi}_2\text{O}_3$ are shown in Table 3 together with those calculated from the known structure of the substance. The structure has been determined by X-ray single crystal technique to a conventional R value of 0.09.¹⁵ It may be concluded from this comparison that in favourable situations it is possible to obtain structure factors of considerable accuracy by this technique. No orientation effects are detectable in this powder pattern. On the other hand the overlaps in the pattern make it impossible to resolve the individual structure factors in most cases. An R value defined as $\sum(F_{\text{calc}}^2 - F_{\text{obs}}^2) / \sum F_{\text{calc}}^2$ was calculated to 0.15. Overlap peaks were included as the sums of their contributions.

Table 3. Guinier powder pattern for α -Bi₂O₃ with observed and calculated intensities. The intensities are corrected for the PLG-factor. Radiation used: CuK α ₁, $\lambda = 1.54051$ Å. $\Delta = 10^5 (\sin^2 \theta_{\text{obs}} - \sin^2 \theta_{\text{calc}})$. p = multiplicity factor.

Lattice parameters:
Present work

$a = 5.8478$ (3) Å
 $b = 8.1673$ (6) Å
 $c = 7.5102$ (4) Å
 $\beta = 112.979$ (4)°

Malmros¹⁵

$a = 5.8486$ (5) Å
 $b = 8.1661$ (10) Å
 $c = 7.5097$ (8) Å
 $\beta = 113.000$ (10)°

h k l	$\sin^2 \theta_{\text{obs}}$ $\times 10^5$	$\sin^2 \theta_{\text{calc}}$ $\times 10^5$	Δ	$ F ^2_{\text{calc}}$	$p F ^2_{\text{calc}}$	$ F ^2_{\text{obs}}$
011	2129	2130	-1	17	66	71
-111	2934	2933	1	28	164	114
110		2936		13		
020	3558	3558	0	76	152	189
-102	4521	4522	-1	371	741	864
021	4798	4799	-1	20	78	75
002	4962	4964	-2	1095	2190	2337
-112	5414	5412	2	518	3709	3543
111		5422		410		
-121	5600	5601	-1	1086	11831	7690
120		5605		1871		
012	5852	5853	-1	723	2893	3138
-211	7831	7829	2	179	714	727
-122		8080		729		
121	8088	8090	-2	725	5816	5789
-202	8178	8174	4	1669	7369	5404
200		8188		2015		
022	8521	8522	-1	256	1023	1108
-212	9065	9063	2	550	2630	2675
210		9077		108		
031	9245	9246	1	346	1384	1355
102	9500	9500	0	599	1198	1190
-131	10049	10048	1	158	1041	1060
130		10052		102		
-113		10372		230		
112	10384	10389	-5	536	3064	3405
-222	11732	11732	0	289	1162	1386
220		11745		1		
-132		12527		77		
131	12535	12537	-2	182	1037	1331
-213	12782	12780	2	229	1140	1414
211		12807		56		
-123		13040		38		
122	13057	13058	-1	478	2066	2042
040	14228	14231	-3	161	322	291
023	14727	14727	0	429	1715	1999
-223		15448		297		
041	15467	15472	-5	1765	8254	7376
221		15475		2		
-232		16179		92		
230	16190	16193	-3	46	552	569
-141	16276	16274	2	3	855	687
140		16278		211		

Table 3. Continued.

-312		16809		499	2650	2400
-311	16816	16819	-3	163		
-104	16925	16925	0	2137	4274	5349
-133	17496	17488	8	308	2496	2415
132		17505		316		
-114		17815		55		
113	17838	17839	-1	621	2704	2934
-204		18088		16		
202	18124	18129	-5	171	375	326
-142	18749	18753	-4	145	633	589
141		18763		13		
-214		18978		259		
212	19011	19019	-8	775	4136	4340
033	19173	19174	-1	864	3849	3978
042		19195		99		
-322	19481	19477	4	944	7052	6099
-321		19488		819		
-233		19895		430		
231	19913	19922	-9	930	5439	5168
014	20746	20746	0	99	397	538
-241	21169	21171	-2	1739	6957	6182
-224	21651	21646	5	1054	5560	5962
222		21687		336		
-323		21949		97		
320	21979	21980	-1	900	3989	3762
-242	22405	22405	0	123	598	679
240		22419		26		
-304		23345		1468		
024	23397	23414	-17	890	6495	7835
-143	23711	23714	-3	976	4332	4509
142		23731		107		
-314		24235		252		
-151	24277	24279	-2	73	4494	4473
150		24283		96		
311		24286		702		
-134	24935	24930	5	99	596	703
133		24954		50		
043	25414	25400	14	60	241	267
-234		26093		6		
-243		26121		189		
232	26141	26134	7	42	3865	3381
241		26149		729		
-333	26398	26396	2	651	3218	3134
330		26427		154		
-152		26758		172		
151	26769	26768	1	327	1998	1814
104	26885	26881	4	1180	2783	3762
-324		26903		106		
213		27713		93		
-115		27739		62	2726	3256
-402	27750	27759	-9	1055		
114		27770		0		
-412	28658	28649	9	87	348	243
-251	29166	29176	-10	81	323	247
-225	30344	30326	18	662	3999	5318
223		30381		337		
302	30862	30853	9	196	392	306
-144		31156		61		

Table 3. Continued.

143	31180	31180	0	630	2764	2741
-153		31719		303		
152	31733	31736	-3	472	3743	3656
312		31742		161		
015	31914	31915	-1	275	1098	1807
-244	32320	32319	1	135	771	683
242		32360		58		
-343	32634	32622	12	283	1515	2176
340		32653		96		
400	32750	32751	-1	1027	2054	1673
053	33407	33405	2	133	534	428
-414		33585		158		
410	33629	33640	-11	281	1756	1453
-161		34063		958		
160		34067		303		
044	34081	34087	-6	118	7103	6633
-253		34126		397		
025	34587	34583	4	490	1958	2042
233		34828		610		
-135	34843	34855	-12	116	3596	3468
134		34886		173		
-432	35767	35764	3	192	768	577
-424	36255	36253	2	613	2451	2156
-162		36542		30		
161	36556	36552	4	713	3043	2718
062		36984		3		
-433		36991		167		
-431	37019	37019	0	107	1109	1335
204	37999	37999	0	181	363	503
-216		38820		88		
332	38861	38858	3	352	1913	3114
214		38889		39		
153		39185		300		
-106	39226	39257	-31	815	2829	4520
-116		40146		317		
115	40175	40184	-9	201	3041	3146
-262		40194		48		
260		40207		194		
350	40678	40658	20	260	3677	4689
-306		40699		1120		
-434		40701		99		
243		41054		42		
-145	41077	41081	-4	1124	4701	4403
144		41111		10		
-226		41489		645		
-163	41507	41502	5	265	3642	5714
162		41519		1		
-425	42436	42445	-9	602	2407	1701
063		43189		507		
-443	43227	43217	10	287	6839	5522
-441		43245		916		
-263	43915	43910	5	467	2338	1653
261		43937		117		
-513		44565		38		
-512	44581	44582	-1	216	1016	848
-345	45020	45012	8	1252	5008	4964

In Fig. 3 a small part of the transmission curve and the corresponding intensity curve from α - Bi_2O_3 are shown. The integrated areas shadowed in Fig. 3 are denoted by zeros on the corresponding curves produced on the line printer. This makes it possible to judge the integration procedure and the definition of the background level for the various peaks.

At $\theta = 23.7^\circ$ (cf. Fig. 3) a double peak corresponding to $\sin \theta = 0.1619$ and 0.1628 , respectively, is seen. Although the sum of the intensities from these lines may be fairly correct they are not well resolved. It might be possible to resolve the intensities by Fourier techniques in the present case. However, considering the usually occurring orientation effects, overlaps, variation in line profiles with θ etc. it does not seem worth-while to include such a procedure at the present stage.

Acknowledgements. The authors are indebted to Professor Peder Kierkegaard for his active interest in this work and for all facilities placed at their disposal. Thanks are also due to Mr. Karl-Erik Johansson for his construction of the film cassette used in this work and to Dr. Don Koenig for his correction of the English of this paper.

This work has received financial support from the *Tri-Centennial Fund of the Bank of Sweden* and from the *Swedish Natural Science Research Council*.

REFERENCES

1. Hägg, G. *Rev. Sci. Instr.* **18** (1947) 371.
2. Westman, S. and Magnéli, A. *Acta Chem. Scand.* **11** (1957) 1587.
3. Klug, H. P. and Alexander, L. E. *X-Ray Diffraction Procedures for Polycrystalline and Amorphous Materials*, Wiley, New York 1954.
4. SAAB. *Film Scanner Manual*, 1967.
5. Abrahamsson, S. *J. Sci. Instr.* **43** (1966) 931.
6. Werner, P.-E. *Arkiv. Kemi* **31** (1969) 505.
7. IBM 1800 *Assembler Language* (Manual 1966).
8. IBM 1800 *Multiprogramming Executive Operating System* (Manual 1972).
9. Arndt, U. W. and Willis, B. T. M. *Single Crystal Diffractometry*, University Press, Cambridge 1966.
10. Sas, W. H. and De Wolff, P. M. *Acta Cryst.* **21** (1966) 826.
11. Werner, P.-E. *Arkiv. Kemi* **31** (1969) 513.
12. Werner, P.-E. *J. Sci. Instr. (J. Physics E)* **4** (1971) 351.
13. Parrish, W. *Acta Cryst.* **13** (1960) 838.
14. Swanson, H. E., Gilfrich, N. T. and Ugrinic, G. M. *Standard X-Ray Diffraction Powder Patterns*, NBS Circular 539, V, **21** (1963) 37.
15. Malmros, G. *Acta Chem. Scand.* **24** (1970) 384.

Received September 1, 1972.